International Journal of Biological Macromolecules 179 (2021) 388–397

Contents lists available at ScienceDirect

International Journal of Biological Macromolecules

journal homepage: http://www.elsevier.com/locate/ijbiomac

Striated myosin heavy chain gene is a crucial regulator of larval myogenesis in the pacific oyster *Crassostrea gigas*

Huijuan Li [a], Hong Yu [a,b], Qi Li [a,b,c,*]

[a] Key Laboratory of Mariculture, Ministry of Education, Ocean University of China, Qingdao 266003, China
[b] Laboratory for Marine Fisheries Science and Food Production Processes, Qingdao National Laboratory for Marine Science and Technology, Qingdao 266237, China
[c] Laboratory of Tropical Marine Germplasm Resources and Breeding Engineering, Sanya Oceanographic Institution, Ocean University of China, Sanya 572000, China

ARTICLE INFO

Article history:
Received 27 November 2020
Received in revised form 2 March 2021
Accepted 3 March 2021
Available online 6 March 2021

Keywords:
CRISPR/Cas9
Crassostrea gigas
Myogenesis

ABSTRACT

Pacific oyster (*Crassostrea gigas*), the most productive economical bivalve mollusc, is identified as an attractive model for developmental studies due to its classical mosaic developmental pattern. Myosin heavy chain is a structural and functional component of myosin, the key muscle protein of thick filament. Here, full length cDNA of striated myosin heavy chains in *C. gigas* (CgSmhc) was obtained, and the expression profiles were examined in different development stage. CgSmhc had a high expression level in trochophore and D-shaped stage during embryo-larval stage. In adult, CgSmhc was a muscle-specific gene and primarily expressed in muscle tissues. Then, activity of 5′ flanking region of CgSmhc were examined through an reconstructed EGFP vector. The results indicated that 3098 bp 5′-flanking region of CgSmhc owned various conserved binding sites of myogenesis-related regulatory elements, and the 2000 bp 5′-flanking sequence was sufficient to induce the CgSmhc expression. Subsequently, the CRISPR/Cas9-mediated target disruption of CgSmhc was generated by co-injection of Cas9mRNA and CgSmhc-sgRNAs into one-cell stage embryos of *C. gigas*. Loss of CgSmhc had a visible effect on the sarcomeric organization of thin filaments in larval musculature, indicating that CgSmhc was required during larval myogenesis to regulate the correct assembly of sarcomere.

1. Introduction

Sarcomere is the basic contractile unit in skeletal and cardiac muscles. The correct assembly of sarcomere is a step-wise process involving hundreds of muscle proteins, and defective sarcomere organization result in muscle-related diseases including muscular dystrophies and cardiomyopathies [1]. The sarcomere is mainly composed of thick and thin filaments made up of myosin and actin, respectively [2]. The myosin molecule is a hexamer consisting of a pair of myosin heavy chains (MHC), a pair of myosin regulatory light chains (MRLC) and a pair of myosin essential light chains (MELC) [3]. N-terminal of myosin is a globular head composed of two MRLCs, two MELCs and part of two MHCs, which own various physiologically functions, such as ATPase activity and actin binding. C-terminal of myosin molecule is a coiled-coil structure called rod consisting of the remainder of the two MHCs, and its function is to convert energy during muscle contraction [4,5].

As a structural and functional component of myosin, myosin heavy chains (MHC) have been widely studied in vertebrates. Various MHC isoforms have been identified in vertebrate skeletal muscles, and each has different primary structures and expression patterns. For instance, there were six fast skeletal MHC isoforms in mammals, of which two isoforms including embryonic and perinatal MHCs were expressed during embryonic, fetal and neonatal; four MHC isoforms including IIa, IIb, IId/x and extraocular MHC had a tissue-specific expression in adult life [6–8]. Besides, the type and number of MHC isoform were corrected with the contractile properties of muscles for the reason that contractile velocity of muscle depends on its myosin ATPase activity [9]. For example, muscle fibers with MHC-IIb showed a faster contractility than MHC-IIa [10]. Current research focused not only on the type and expression pattern of MHC, but also on its genetic functions. In mice, genetic mutation of MHC-IIb or -IIx resulted in weighed less, muscle weakness and interstitial fibrosis. At the meantime, the MHC-IIb null mice showed a significantly reduced levels of muscle contractile force [11]. In zebrafish, knockout of slow myosin heavy chain 1 resulted in disrupted sarcomere organization and reduced larval locomotion in embryonic slow muscle [12]. The deletion of certain cis-acting elements and transcription factor binding sites in 5′ flanking region of MHC, such as MRFs, MyoD, Mef2 and Pax3, reduced the MHC expression, indicating that MHC promoter might be involved in muscle growth in fish [13].

Although Mollusca is the second group in invertebrate, the function of MHC in mollusc is poorly understood compared with vertebrate counterparts, only fragmental data is available about molluscan MHCs.

* Corresponding author at: Key Laboratory of Mariculture, Ministry of Education, Ocean University of China, Qingdao 266003, China.
E-mail address: qili66@ouc.edu.cn (Q. Li).

https://doi.org/10.1016/j.ijbiomac.2021.03.022
0141-8130/

MHCs cDNA sequence have been obtained in various mollusks including scallops *Argopecten*, *Patinopecten*, *Pecten*, *Placopectin* and squid *Loligo* [14–18]. Scallop and squid had four and two MHC isoforms alternatively spliced from a single gene, respectively [17,18].

The Pacific oyster, *Crassostrea gigas*, is the most productive economical shellfish in the world. Because of its unique living environment and developmental pattern, *C. gigas* have gradually attracted a great of attention and became the models in researches on ocean acidification, immunity, biomineralization and developmental biology [19]. Similarly to most mollusc, the researches on *C. gigas* muscle just focus on macro muscle type and muscle function. For instance, the adductor of *C. gigas* was composed of two parts including the striated phasic adductor and smooth tonic adductor (catch muscle). Among these, the striated adductor was responsible for quick closure of the valves, whereas the smooth adductor participated in holding the shells tightly shut for long periods [20]. Previously, we have revealed a dynamic pattern of myogenesis during embryonic and larval development in *C. gigas* [21]. However, due to the lack of effective tools to study the gene function, the molecular mechanism of muscle growth and development during embryonic or adult life is still obscure in *C. gigas*.

Reverse-genetics are important approach to explore gene function and genetic engineering. In mollusc, RNA interference (RNAi) technology is usually used to investigate the functions of genes. RNAi technology only knockdown gene to affect the gene translation rather than a complete loss-of-function knockout. Hence, trait associated genes can't be accurately targeted due to the insufficient knockdown [22]. Recently, CRISPR (clustered regularly interspaced short palindromic repeats)/Cas9 system is known as the most promising and versatile gene editing tool [23]. CRISPR/Cas9 technology has been successfully applied in both model and non-model species including zebrafish, mice, Atlantic salmon, jellyfish, sea urchin and hydra [24–29]. However, there are few research on the application of CRISPR/Cas9 system on marine bivalves. In *C. gigas*, we have previously reported that efficient induction of indel mutations in two target gene (MSTN and Twist) in *C. gigas* after delivering the complex of sgRNA and Cas9 protein into embryos. However, no phenotype was detected [30].

In present study, we obtained the full length cDNA of the striated myosin heavy chains in *C. gigas* (CgSmhc) and examined its expression profiles in different embryo-larval development stage and different adult tissues. Furthermore, we investigated the 5′ flanking regions of CgSmhc and analyzed its promoter activity. Finally, we knocked out the CgSmhc by CRISPR/Cas9 to examine its role in embryonic and larval myogenesis in *C. gigas*. Our results would enable us to better understand the function of MHC in mollusc and provide a foundation for studying the molecular mechanisms of muscle growth and development. On the other hand, our study also provided a powerful tool for genetic engineering to increase important economical traits of oyster for aquaculture.

2. Materials and methods

2.1. cDNA synthesis and bioinformatic analysis

Total RNA of samples from different adult tissues and different embryo-larval development stages were extracted with Trizol® reagent (Thermo) according to the manufacturer's instructions. The total RNA was reverse transcripted into cDNA by PrimescriptTM Reverse Transcription Kit (Takara). The 3′ and 5′ cDNA were cloned by SMARTer® RACE 5′/3′ Kit (Clontech). The internal fragment and 3′/5′ terminal PCR reactions were amplified with PrimeSTAR® Max DNA Polymerase (Takara) and Tks Gflex™ DNA Polymerase (Takara). Specific primer sequences used in the amplification were listed in Table 1.

The 3′/5′ terminal and internal fragment were assembled using SeqMan (DNAStar) to acquire the full length cDNA of CgSmhc. The open reading frame was predicted by the ORF finder of NCBI (https://www.ncbi.nlm.nih.gov/orffinder/). The deduced amino acid sequence was analyzed with the DNAMAN (Lynnon Biosoft). The molecular weight (MW) and isoelectric point (pI) of deduced amino acid sequences were predicted using the Compute pI/MW Tool at the ExPAsy site (http://web.expasy.org/compute_pi/). The protein sequence alignment was conducted using the ClustalW (Lynnon Biosoft, Los Angeles, CA) and modified by ESPript 3.0 [31]. The conserved domains were predicted with the CD-Search tool of NCBI (https://www.ncbi.nlm.nih.gov/Structure/cdd/wrpsb.cgi). A phylogenetic tree was constructed by the Neighbor-Joining analysis with 1000 bootstrap replicates using MEGA 7.0 software [32].

Table 1
Specific primers used in this study.

Primer name	Sequence(5′-3′)	Usage
CgSmhc-5′RACE	GGCTCAGCGGTTCCGTCCACCTCAG	RACE
CgSmhc-3′RACE	GACAAGACCGTCCAGGAATGGCAGAGCA	RACE
CgSmhc-1F	TTGAAGCCTACGGAAACGC	Fragment amplication
CgSmhc-1R	TCTTACCGCCACCCTCTTCT	Fragment amplication
CgSmhc-2F	GTCATTACGCTGGCTCTGTG	Fragment amplication
CgSmhc-2R	CCAAGTTGTCTTCCATCTCATC	Fragment amplication
CgSmhc-3F	CCTTGATGAGGAAGACGCTG	Fragment amplication
CgSmhc-3R	CTTGCTCTTTCAGCGGATTC	Fragment amplication
RT-Smhc-F	GATTACTGGTGAGTCTGGAGCCG	RT-qPCR specific primer
RT-Smhc-R	CTTCATCCTTCTTTTGCTGTCCA	RT-qPCR specific primer
EF1α-F	AGTCACCAAGGCTGCACAGAAAG	RT-qPCR internal control primer
EF1α-R	TCCGACGTATTTCTTTGCGATGT	RT-qPCR internal control primer
CgSmhc-ISH-F	TTCGGCTGGTTGGTCAAGAGAG	ISH
CgSmhc-ISH-R	GATCACTAATACGACTCACTATAGGGATG AGGGTGAGTGCTGTACAAGTTC	ISH
P3098-F	CCCAAGCTTTTCAACACTGTGACCTGATG GAATC	5′-Flanking region amplification
P2000-F	CCCAAGCTTATCTCTCTCGATCTCTGATTGG CT	5-Flanking region amplification
P-R	CGCGGATCCGGGACCCAGCACATCTTCTTG	5-Flanking region amplification
CgSmhc-sgRNA-1	GATCACTAATACGACTCACTATAGGGCTG GGTCCCCGACGAGA GTTTTAGAGCTAGAAAT	sgRNA synthesis
CgSmhc-sgRNA-2	GATCACTAATACGACTCACTATAGGAGAG CCTGGCCGTAGATG GTTTTAGAGCTAGAAAT	sgRNA synthesis
CgSmhc-sgRNA-R	AAAAGCACCGACTCGGTGCC	sgRNA synthesis

2.2. RNA expression analysis of CgSmhc by real-time quantitative PCR

To characterize the expression of CgSmhc during *C. gigas* embryonic and adult development stages, we quantified the transcript levels of CgSmhc in different embryo-larval developmental stages and different adult tissues by RT-qPCR. The qPCR was amplified using SYBR® Premix ExTaq™ II kit (Takara) on a LightCycler® 480 real-time PCR system (Roche) according to the manufacturer's protocols. The specified primers were designed, and its specific was detected by conventional PCR and melting curve analyses. Elongation factor 1-α (EF1-α) and Ribosomal protein S18 (RS18) were the internal control primers in the adult samples and larvae, respectively [33]. The relative expression was calculated by the $2^{-\Delta\Delta CT}$ method. All data and the significant differences were analyzed using the IBM SPSS Statistics 22 by one-way ANOVA followed by a multiple comparison. Differences were considered statistically significant at $P < 0.05$.

2.3. RNA location pattern analysis of CgSmhc by in situ hybrization

Whole mount in situ hybridization (WISH) and tissue in situ hybrization (TISH) were used to analyze the RNA location pattern in different embryo-larval and different adult tissues, respectively. The digoxigenin-labeled sense and anti-sense probes synthesized following T7-mediated in vitro transcription (MEGAscript kit, Ambion) using a DIG-RNA labeling Kit (Roche) from the cDNAs fragment of target genes. The specific primers were showed in Table 1. The WISH was conducted using the protocol described by Thisse with some modification [34]. After PBST rehydration, the samples were prehybridized in hybridization buffer (50% formamide, 50 μg/ml of heparin, 5 × SSC, 500 μg/ml tRNA, 0.1% Tween-20, 9.2 mM citric acid) at 65 °C for 6 h. The sense and anti-sense probes were added to the samples and hybridized to target overnight at 65 °C. After samples were rinsed with low salt and blocking buffer, the anti-digoxigenin antibody (Roche) at 1:5000 in blocking solution was added. Color reactions were performed with 2% NBT/BCIP solution (Roche) for 2–6 h at room temperature.

According to the results of RT-qPCR, striated adductor muscle, smooth adductor muscle and mantle were selected as the sample of TISH. 5 μm paraffin sections were chose to perfume the experiment. After deparaffinized, prehybridization, hybridization and antibody incubation, the sections were incubated in 2% NBT/BCIP solution (Roche) for 2–12 h at room temperature. When the specific signal was detected, the sections were re-stained with 0.5% eosin.

2.4. 5′-Flanking region amplification and recombinant plasmid construction

To identify the minimal promoter, different length 5′-flanking region of CgSmhc were fused to EGFP in pEGFP-1 reporter vector. Three 5′ deletion constructs within the 3098 bp flanking region from the start codon of CgSmhc were generated using *C. gigas* genomic DNA as a template. The constructs were named as P3018, P2000 and P1374, where the numbers represented the nucleotide positions upstream of the CgSmhc start codon (Fig. 4). The DNA fragments of P3018 and P2000 were amplified by Tks Gflex™ DNA Polymerase (Takara) and then cloned into the BamHI-*Hin*dIII site of the pEGFP-1 reporter vector (www.miaolingbio.com). The PCR primers were showed in Table.1. The P1314 construct vector was generated by cutting P3018 with *Sac* I endonuclease. All constructs were confirmed by sequencing and contained a CgSmhc flanking region conjugated with the EGFP reporter gene and SV40 ployA signal (Fig. 4). Transcription factor-binding sites in the 5′-flanking region of CgSmhc were predicted by JASPAR (http://jaspar.genereg.net/search?advanced=true).

2.5. Preparation of sgRNA and Cas9 mRNA

Two sgRNA target sites named CgSmhc-sgRNA-1 and CgSmhc-sgRNA-2 were designed using an online tool CRISPOR (http://crispor.tefor.net/). CgSmhc-sgRNA-1 and CgSmhc-sgRNA-2 were located in second and third exon of CgSmhc (Fig. 5-I). The SgRNAs were synthesized using the MEGAshortscript T7 Transcription Kit (Thermo Fisher Scientific). The synthesized sgRNAs were purified by phenol chloroform extraction and stored in aliquots at −80 °C. The pT3TS-nCas9n plasmid was linearized by *Xba* I (NEB) and purified by phenol/chloroform extraction. The purified linearized plasmid was used as the template to synthesize capped Cas9 mRNA using T3 RNA polymerase kit (Ambion). Then, it was purified by phenol chloroform extraction for microinjection.

2.6. Microinjection

Each EGFP reporter constructs was diluted to 150 ng/μl with sterile distilled water containing 0.5% phenol red and delivered into one-cell *C. gigas* embryos using a Warner PLI-100A Pico-Injector microinjector (Warner Instruments). The injected embryos were incubated in filtered seawater at 24 °C, and subjected to observation of EGFP expression profiles during development under a fluorescence light microscope (Olympus BX53) with digital camera (Olympus DP73). The Cas9 mRNA and sgRNAs were diluted with Cas9 working buffer (0.5% phenol red, 20 mM HEPES and 150 mM KCl) at 500 ng/μl, respectively. Approximately 0.1 nl of sgRNA/Cas9 solution was injected into one-cell stage embryos. The injected embryos were incubated in filtered seawater at 24 °C.

2.7. DNA extract and indels detection by Sanger sequencing

The genomic DNA was extracted from D-shaped larvae using Chelex®-100 method [35]. The genomic region flanking the target site was amplified with 2× Taq Plus Master Mix II (Dye Plus) (Vazyme) according to the manufacturer's instruction. The PCR fragments were purified and then cloned into pMD19-T Simple Vector (Takara). Twelve clones were randomly selected for DNA sequencing using M13F primer.

2.8. RNA expression analysis of larvae with CgSmhc knockout

RT-qPCR was used to investigate the effect of the knockout at the mRNA level. The larvae total RNA was extracted using MicroElute Total RNA Kit (Omega) according to the manufacturer's instructions. The total RNA was reverse transcripted into cDNA by HiScript III 1st Strand cDNA Synthesis Kit (Vazyme). The qPCR was amplified using ChamQ SYBR Color qPCR Master Mix (Vazyme) on a LightCycler® 480 real-time PCR system (Roche) according to the manufacturer's protocols. The specific primer and internal control primer were showed in Table.1. The relative expression was calculated by $2^{-\Delta\Delta CT}$ method. All data and the significant differences were analyzed using the IBM SPSS Statistics 22. Differences were considered statistically significant at $P < 0.05$.

2.9. Phonotype screening

Phalloidin staining was used to characterize the musculature in wild type and injected larvae. The method was performed as previously reported [21]. Briefly, samples were anesthetized with 7.5% $MgCl_2$, and then fixed in 4% PFA in 0.1 M PBS for 2 h at room temperature. The fixed larvae were de-calcification in 0.5 M EDTA for 3–5 h at room temperature, and the larvae were transferred into the PBS containing 2% Triton-X 100 (PBT, pH = 7.3). Phalloidin-iFluor™ 488 Conjugate (AAT Bioquest) in a 1:1000 dilution in PBT was used to label larval musculature. Image acquisition and analysis were performed on an ultra-high-resolution laser confocal microscope Leica TCS SP8 STED 3× equipped with Leica Application Suite X software. Confocal image stacks were recorded with 1.5–3 μm step size along the *Z*-axis and merged as maximum intensity projections.

3. Results

3.1. cDNA cloning and sequence analysis of CgSmhc

The nucleotide and deduced amino acid sequences of CgSmhc were shown in Attachment 1. The full-length cDNA of CgSmhc was 6410 bp, containing a 5′-untranslated region (5′-UTR) of 195 bp, a 3′-untranslated region (3′-UTR) of 388 bp, and a putative open reading frame (ORF) of 5827 bp encoding a 1942-amino acid protein with an ATG start codon and TGA stop codon. A polyadenylation signal, AATAAA, was found 19 bases upstream from the poly (A) tail. The predicted molecular mass and the isoelectric point of CgSmhc were 223.17 kDa and 5.57, respectively. The CgSmhc protein contained Myosin_N, MYSc, IQ and Myosin_tail_1 conserved domains predicted by SMART software. The putative protein secondary structure of CgSmhc contained 77% alpha helices, 3% beta strand structures and 1% TM helix (Fig. 1-I). The tertiary structure of MHC protein was based on template1kk8.1.A, which shared 81.81% identity with CgSmhc protein (Fig. 1-II).

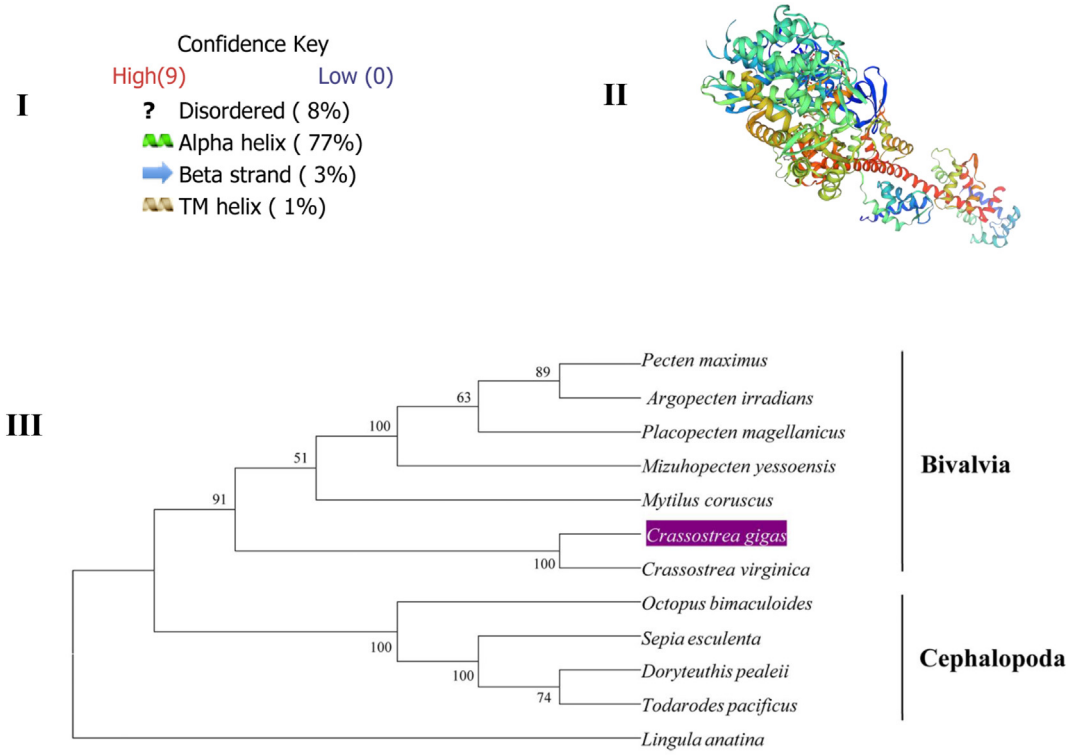

Fig. 1. I: the predicted second structure of the CgSmhc protein. The putative protein secondary structure of CgSmhc contained 77% alpha helices, 3% beta strand structures and 1% TM helix; II: The predicted three-dimensional structure of the CgSmhc protein; III: Neighbor-joining phylogenetic tree based on the amino acid sequences of CgSmhc. Numbers at tree nodes refer to percentage bootstrap values after 1000 replicates.

3.2. Homology and phylogenetic analysis of CgSmhc

The amino acid sequence alignment of CgSmhc with Smhc from other Mollusca species available on GenBank (*Crassostrea virginica*, XP_022323361.1; *Pecten maximus*, XP_033742439.1; *Mytilus coruscus*, CAC5402204.1; *Argopecten irradians*, P24733.1; *Placopecten magellanicus*, P24733.1; *Mizuhopecten yessoensis*, XP_021367471.1; *Octopus bimaculoides*, CDG41623.1; *Doryteuthis pealeii*, AAC24207.1; *Sepia esculenta*, ACD68202.1; *Todarodes pacificus*, ADU19853.1). The alignment results revealed that Smhc exhibited a high similarity level of sequence conservation (70.99–95.06%) among Mollusca species (Attachment 2). It showed the highest similarity to Smhc of genus *Crassostrea* such as *Crassostrea virginica* (95.06%). A high sequence similarity was detected in other Bivalva species such as *A. irradians* (75.38%), *P. maximus* (75.27%), *P. magellanicus* (74.91%), *M. yessoensis* (74.92%), 74.92%, *M. coruscus* (73.80%). A high sequence similarity was also found in Cephalopoda species such as *O. bimaculoides* (72.1%), *S. esculenta* (71.58%) and *D. pacificus* (70.99%). Some motifs in CgSmhc including ATP binding sites, switch I/II region, converter subdomain, relay loop and SH1 helix were conserved among Mollusca species (Attachment 2). The phylogenetic analysis of CgSmhc indicated that all Bivalva species were clustered together and formed three branches, genus *Crassostrea, Mytilus and* genus scallop (Fig. 1-III). *Crassostrea* species was clustered together, and was closely related to the *M. coruscus*. Cephalopoda species were clustered together as another independent branch.

3.3. Temporal expression patterns of CgSmhc

In adult, CgSmhc was identified as a muscle-specific gene and primarily expressed in muscle tissues including striated adductor muscle, smooth adductor muscles and mantle (Fig. 2-I). CgSmhc exhibited the highest expression level in striated adductor muscle, and relatively weakly in the smooth adductor muscle and mantle. CgSmhc mRNA was not detected until blastula stage ($P < 0.05$) during the embryo-larval developmental stages (Fig. 2-II). CgSmhc transcript levels increase sharply from trochophore stage, peaking at D-shaped stage, declining thereafter until umbo larvae and eyed larvae stages ($P < 0.05$).

3.4. RNA localization patterns of CgSmhc

In adult, the localization of specific signal in striated adductor muscle was significantly stronger than that in smooth adductor muscle (Fig. 3-I). In mantle, the specific staining was detected in columnar epithelium. In addition, the specific signal was identified in the sarcomere structure in striated adductor muscle and mantle columnar epithelium (Fig. 3-I-D, -I-H). Similarly to results of RT-qPCR, the RNA localization of CgSmhc was restricted on muscle tissues during embryonic-larval development stages (Fig. 3-II). In gastrula stage, a stained cell cluster was detected at the middle of embryo. The cell cluster have an increase in number and size and grows into a number of clusters, eventually forming a muscle ring in trochopore stage. In D-shaped larvae stage, the specific staining gradually formed a regular pattern, which was located in larval velum retractor and adductor muscles. The specific signals was identified in velum retractor, anterior and posterior adductor muscles during umbo and eyed larvae stages. There was a regular pattern of transverse striation structure in the velum retractor muscle during umbo and eyed larvae stage (Fig. 3-II).

3.5. Structure prediction and analysis of the 5′ flanking regions of CgSmhc

The first base in the ATG start codon of CgSmhc was labeled as +1, and a series of putative binding sites of myogenesis-related transcription factors were screened within the 3098 bp sequence (Fig. 4-I). There were four growth factor independent transcriptional repressor (GFI), four Myocyte-specific enhancer binding factor 2 (Mef-2), one LIM homeobox domain transcription factor (ISL), one Myogenic factor 5 (Myf-5), two nuclear factor of activated T cells (NFAT), one serum

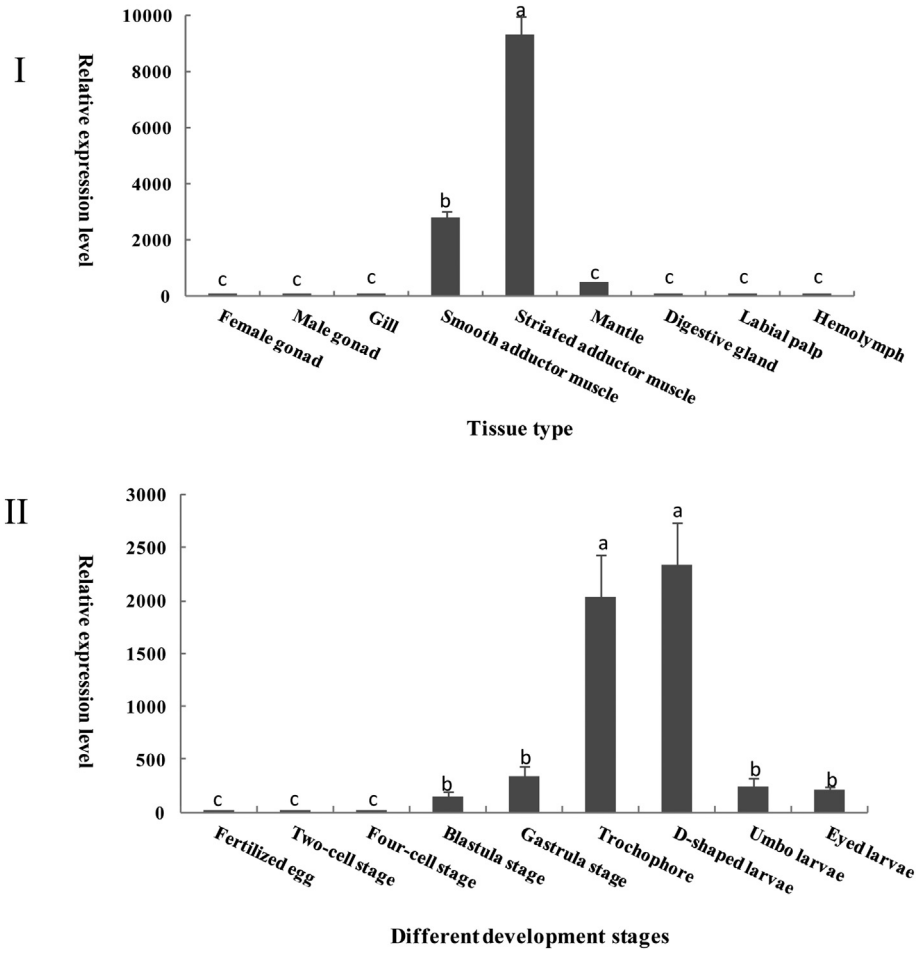

Fig. 2. Expression profiles of CgSmhc. I: Expression characterization of CgSmhc in various adult tissues; II: Expression profiles of CgSmhc during embryo-larval developmental stages. Different letters indicated significantly different ($P < 0.05$).

response factor (SRF) and three TATA box binding sites. One GFI, Two Mef-2 and two TATA box binding sites were located between −3000 and −2000; three GFI, one Mef-2, Myf-5, NFAT, SRF and TATA box binding sites were located between −2000 and −1374; one SRF, Mef-2 and NFAT were located between −1374 and +1.

3.6. Activity analysis of the 5′ flanking regions of CgSmhc

To identify the minimal promoter necessary to induce expression of CgSmhc, three recombinant vector namely P3098, P2000 and P1374 were microinjected into one-cell embryos of *C. gigas* as an in vivo reporter assay. There was no difference in expression efficiency and expression pattern for P3098 and P2000. About 80% ($n = 70$) of the injected embryos showed a strong EGFP expression along larval musculature including adductor muscle and velum retractor. The EGFP signal was first detected at 13 h post-fertilization (hpf) in the trochophore stage (Fig. 4-II). The specific signal subsequently detected in various stages from trochophore stage to umbo stage, and the signal gradually strengthened with the extension of the development stage. However, there was no EGFP signal for P1374. These data confirmed that the 2000 bp 5′-flanking region of CgSmhc owned the essential regulatory sequences for muscle-specific expression.

3.7. Identification of effective sgRNA and characterization of indel mutations in the injected embryos

CgSmhc-sgRNA-1 and CgSmhc-sgRNA-2 were mixed separately with Cas9 mRNA and injected into one-cell stage embryos. The final concentration of sgRNAs and Cas9 mRNA were 500 ng/μl. The two sgRNAs were very effective in guiding Cas9 induced mutagenesis, showing evident multiple peaks near PAM sites of the target sequences (Fig. 5-II). The target mutagenesis efficiency of CgSmhc-sgRNA-1 and CgSmhc-sgRNA-2 was 90% and 80%, respectively. In addition, the injected embryos showed no significant difference in viability than un-injected embryos.

The types of indel mutations induced by co-injection of sgRNAs and Cas9 mRNA were identified by sequencing each. The CRISPR/Cas9-induced mutations in CgSmhc-sgRNA-1 and CgSmhc-sgRNA-2 target sites were mainly small indel mutations ranging in size from 1 to 5 bp and 1 to 41 bp, respectively (Fig. 5-III). The types of indel mutations of two target sites were predominantly insertion and deletion. Some of these indel mutations were frame-shift mutations that alter the protein translation and disrupt the gene function.

3.8. Phenotypic evaluation of G0 injected embryos

To assess whether the CgSmhc mutation affected the larval myogenesis, the larval musculature was characterized by phalloidin staining that labels the F-actin thin filaments. Loss of CgSmhc had a visible effect on the sarcomeric organization of thin filaments in larval musculature. The sarcomere structure of larval velum retractor displayed various degrees of abnormality in CgSmhc-sgRNA-1 and CgSmhc-sgRNA-2 injected larvae (Fig. 6B–I). The proportion of larvae with sarcomere defection in CgSmhc-sgRNA-1/Cas9mRNA and CgSmhc-sgRNA-2/Cas9 mRNA injected larvae was 75% and 56%, respectively. This was in conformity with the finding that CgSmhc-sgRNA-1

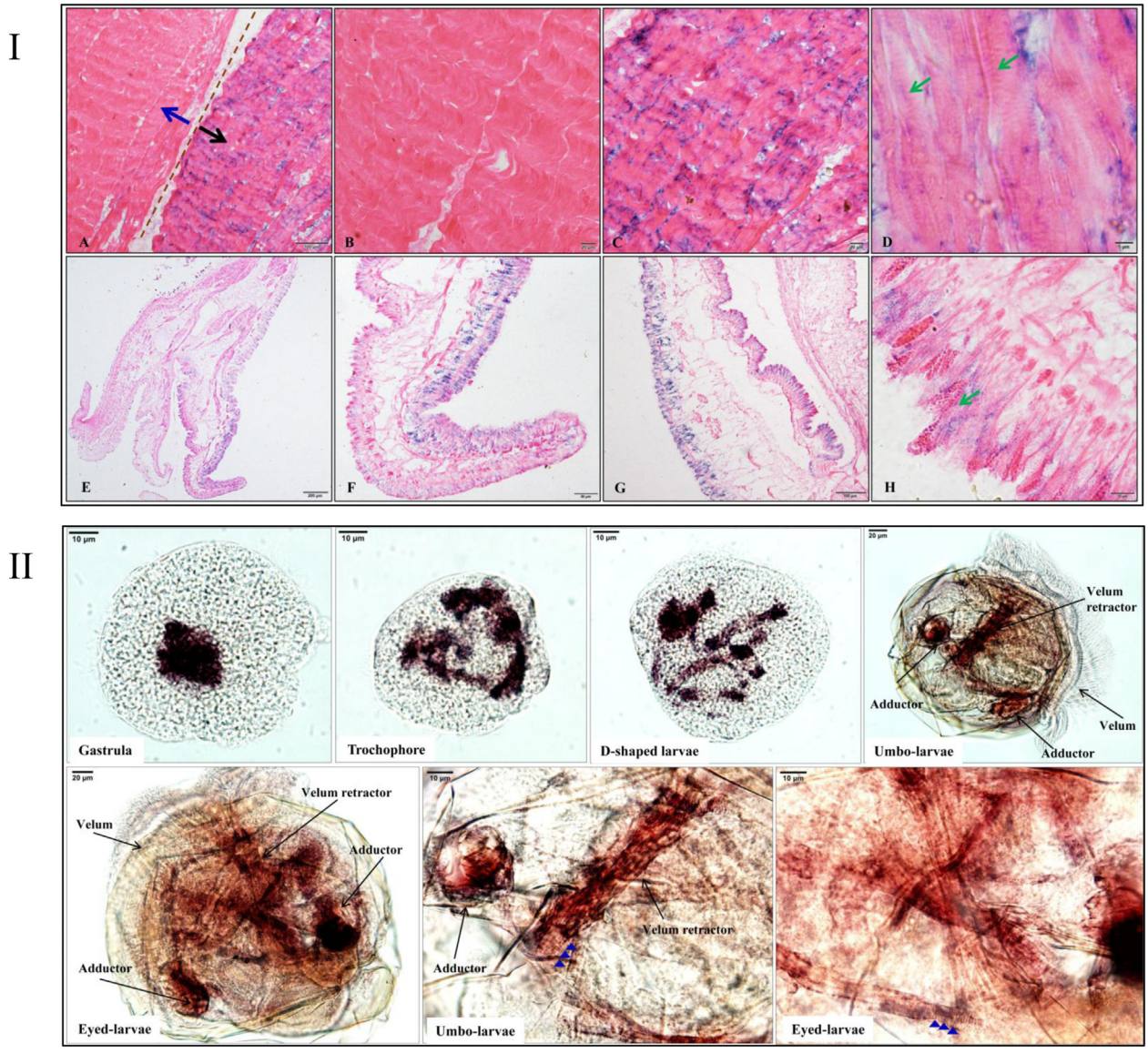

Fig. 3. RNA localization patterns of CgSmhc. I: Expression profiles of CgSmhc in adult muscle tissues. A: adductor muscle; B: Smooth adductor; C–D: Striated adductor; the blue arrow indicates the smooth adductor; the black arrow indicates the striated adductor; the green arrows refer to the striated structure of the striated adductor. E–H: Expression profiles of CgSmhc in adult mantle tissue. The green arrows refer to the striated structure of the mantle tissue. II: RNA localization patterns of CgSmhc during embryo-larval developmental stages. CgSmhc expression profiles were primarily restricted to muscle structures including adductor muscle and larval velum retractors. The blue triangles represent the transverse striations in the larval velum retractor.

was more effective than CgSmhc-sgRNA-2 in guiding Cas9 induced mutagenesis at their respective target sites. To test whether multiple sgRNAs could further enhance the mutation efficiency for phenotype analysis, we combined CgSmhc-sgRNA-1 with CgSmhc-sgRNA-2 and co-injected with Cas9 mRNA into one-cell embryos. 85% of the injected larvae exhibited sarcomere defection. Dual sgRNAs injections not only resulted in an increased proportion of larvae showing sarcomere defection, but also increased the degree of sarcomere abnormality (Fig. 6J–L). In contrast, Cas9 mRNA or sgRNA injection alone had no significant effect on larval musculature compared with control.

Subsequently, to evaluate the effect of the knockout at the mRNA level, we quantified the CgSmhc expression by RT-qPCR. The results showed that the expression of CgSmhc was severely down-regulated in larvae with Cas9mRNA/CgSmhc-sgRNA-1/2 injection (Attachment 3-I). In addition, loss of CgSmhc led to a significant reduction of larval motor ability (Attachment file 4) and larval hatching rate (Attachment 3-II, Table. 2), mainly in swimming distance and speed. In contrast, sgRNA or Cas9 mRNA injection alone showed no significant difference in larval locomotion ability (Attachment file 5).

4. Discussion

4.1. The sequence characteristics of CgSmhc

CgSmhc owned the typical functional domains of myosin heavy chain family, namely MYSc, Myosin_N, IQ and Myosin_tail. The MYSc had large ATPase, and was the molecular motor of myosin. The content and hydrolysis rate of ATPase were closely related to various metabolic and physiological characteristics of muscle, such as the contraction speed and muscle type [36,37]. Therefore, myosin heavy chain was often used to identify the different muscle types. The IQ domain was a basic unit consisting of about 23 amino acids, and its conserved core

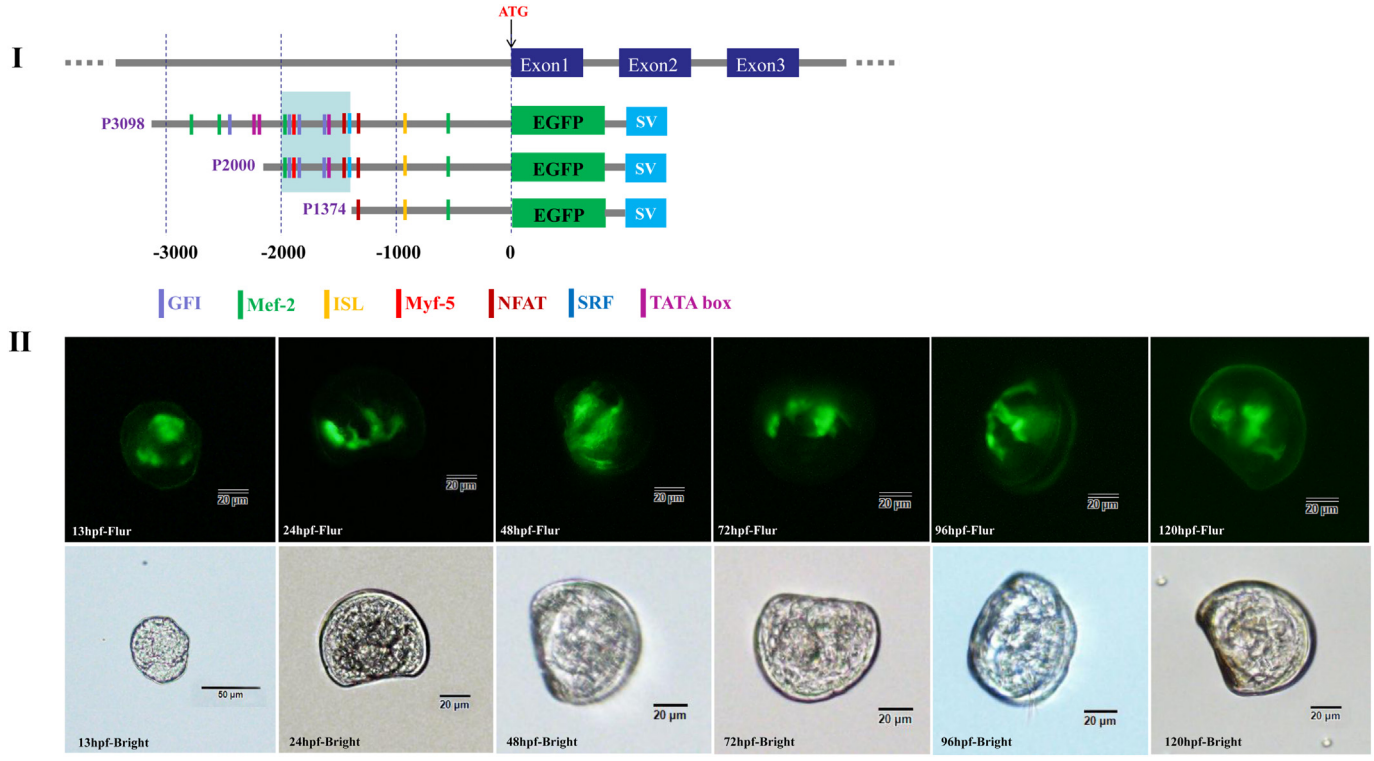

Fig. 4. I: Schematic of reporter constructs used in this study. Putative binding sites of representative myogenesis-related transcription factors, growth factor independent transcriptional repressor (GFI), myocyte-specific enhancer binding factor 2 (Mef-2), LIM homeobox domain transcription factor (ISL), myogenic factor 5 (Myf5); nuclear factor of activated T-cell (NFAT); serum response factor (SRF); TATA box, are plotted on the P1374–P3098 constructs. II: The expression patterns of P2000 during different larval stage. hpf: hours post-fertilization.

fit the consensus A-x(3)-I-Q-x(2)-F-R-x(4)-K-K. The IQ domain served as a binding site for EF-hand family including regulatory and essential light chain, calmodulin [38]. In mollusks, the muscle contraction was triggered by combination of Ca^{2+} and EF hand domains of the MELC [39]. CgSmhc owned the conserved coiled-coil Myosin_tail region. The coiled-coli was composed of the tail from two molecules of myosin, which was the structural backbone of thick filaments [40]. From the above, CgSmhc owned the conserved domains that were structurally or functionally important in the myosin heavy chain family.

The multiple sequence alignment of CgSmhc with other Mollusca species showed a high conservativeness (70.99–95.06%). A series of important amino acid sites were identified in alignment sequence, such as ATP binding sites, switch I/II region, converter subdomain, relay loop and SH1 helix. The high sequence similarity indicated the conserved functions of CgSmhc among mollusks. The phylogenetic analysis of CgSmhc indicated that all Bivalva species were clustered together, which was consistent with the traditional taxonomy.

4.2. The temporal expression patterns of CgSmhc

During the embryo-larval developmental stages, CgSmhc transcript level increased significantly from gastrula and trochophore, and reached its peak at the D-shaped larval stage. The expression pattern of CgSmhc was similar to some muscle-related genes in bivalves. For examples, myosin essential light chain in *C. gigas* and twitchin in *Mytilus trossulus* showed a higher expression levels during trochophore and D-shaped larvae stage [41,42]. Previously, we have characterized the myogenesis process during *C. gigas* embryo-larval development stage [30]. The first larval musculature appeared the early trochophore stage, and a well-organized muscle system were established at D-shaped larvae stage. Therefore, the high expression level of CgSmhc in trochophore and D-shaped larvae stage indicated that CgSmhc might be involved in the larval myogenesis in *C. gigas*.

In adult, the expression level of CgSmhc in striated adductor muscle was nearly four-fold higher than smooth adductor muscle. In oyster, the slide between actin and myosin in striated adductor muscle was five times faster than in smooth adductor muscle, resulting in a faster contraction of the striated adductor muscle [29]. Generally, the difference of ATPase activity in myosin heavy chain head was closely related to the contraction rate of muscle fibers [43,44]. Therefore, we speculated that CgSmhc might be correlated with the muscle contraction in *C. gigas*.

4.3. RNA location patterns of CgSmhc

The specific signal of CgSmhc increased dramatically during trochophore stage, when the larval musculature began to form. The location pattern of CgSmhc was similarity to the larval musculature during D-shaped stage, umbo larvae stage and eyed larvae stage, which was primarily located in the adductor muscle and larval velum retractor. In *C. gigas*, this unique muscle-specific expression profile was also found in myosin essential light chain [41]. Collectively, these data indicated that CgSmhc expression profile was primarily restricted to muscle structures during embryogenesis.

Similar to the data of qRT-PCR, the specific signal of CgSmhc in striated adductor muscle was significantly higher than that in smooth adductor muscle in adult. In *C. gigas*, the striated adductor muscle had a faster contraction rate and was responsible for the quick closure of shell. Therefore, we speculated that CgSmhc was related to the muscle contraction in *C. gigas*. In adult mantle, CgSmhc was located in the columnar epithelium, which rested on connective tissue containing scattered muscle fibers [45]. In addition, the expression signals of CgSmhc was detected in transverse striation structure of muscle fibers

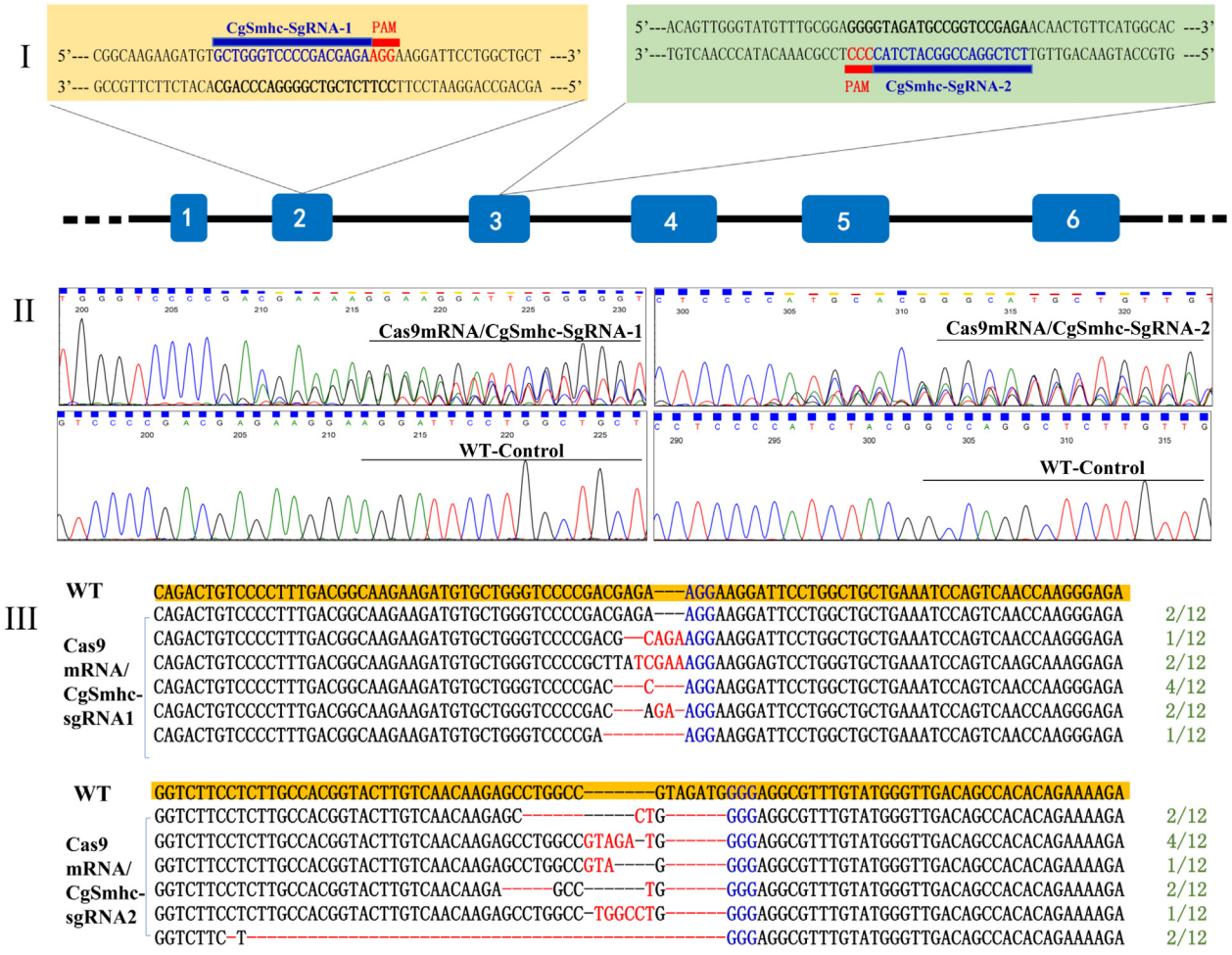

Fig. 5. I: Schematic diagram of CgSmhc-sgRNAs. The PAMs are shown in red, and the sgRNA sequences are shown in bule. CgSmhc-sgRNA-1 and CgSmhc-sgRNA-2 were located in second exon (the sense strand) and third exon (the antisense strand) of CgSmhc. II: Sanger sequencing of PCR products in the injected embryos. WT means the wild type. The CgSmhc-sgRNA-1/2/Cas9 mRNA injected embryos showed evident multiple peaks near PAM sites of the target sequences. III: Sequence characterization of indel mutations in the injected embryos. PAM sequences are shown in blue, and the inserted and deleted nucleotides are shown in red. The green font indicated the numbers of mutated clones identified from all analyzed clones from each sample.

in various muscle tissue including larval velum retractor, adult striated adductor and mantle, indicating that CgSmhc might be involved in the organized sarcomere assembly.

4.4. Structural analysis of the 5′ flanking regions of CgSmhc

The 5′ flanking region of gene was an important transcriptional regulatory region, which mainly included the un-transcribed DNA sequence, as well as promoters, regulatory elements, enhancers and inducible elements [46,47]. A serious of binding sites of myogenesis-related transcription factors within the 3098 bp 5′ flanking regions of CgSmhc were screened, including mainly NFAT, SRF, Mef-2, Myf-5, GFI and TATA box. All of these putative binding sites have been shown to be crucial for transcription activity of MYH in some vertebrate species. For instance, deletion of NFAT binding sites in 5′ flanking regions of MYH resulted in an apparent reduction in the promoter activity in zebrafish [48]. SRF was a transcription factor that bind to serum elements associated with a variety of genes including muscle-specific genes, and influenced muscle development and functions by regulating the expression of muscle-specific gene [49,50]. Previous study indicated that SRF acted as an enhancers of MyHC-IIb transcriptional activity in mice [51]. In zerbrafish, SRF were identified as a critical element of MYH promoter activity [52]. Mef-2 and Myf-5 binding sties were necessary for the expression of MYHs in fish and mammal [52]. Mef-2 binding sites were also involved in transcription regulation of MYHs expression in medaka and common carp [53,54].

4.5. Activity analysis of the 5′ flanking region of CgSmhc

To identify the minimal promoter necessary to induce expression of CgSmhc, three recombinant vector namely P3098, P2000 and P1374 were microinjected into one-cell embryos of *C. gigas* as an in vivo reporter assay. The 2000 bp 5′ flanking region of CgSmhc was sufficient to induce gene expression in *C. gigas*, while 1374 bp 5′ flanking region was not effective. The result indicated that the 5′ flanking region from 2000 to 1314 bp might be an necessary region for CgSmhc expression. The reduced promoter activity for the successive deletion of 5′ flanking region indicated that any or combination of these binding sites might be concerned with the transcriptional regulation of CgSmhc. Similarly, 2100 bp 5′ flanking region of MYH was the minimal promoter necessary to induce gene expression, and 5′ flanking region shorter than 2100 bp lead to a significant reduction in gene expression activity in zebrafish [48]. The EGFP signal of P3098 or P2000 were detected firstly at the trochophore stage, and were mainly located in the larval musculature including adductor and velum retractor. The EGFP expression profile was overlapped with known larval myogenesis progress, indicating that CgSmhc might be involved in larval muscle development in *C. gigas*.

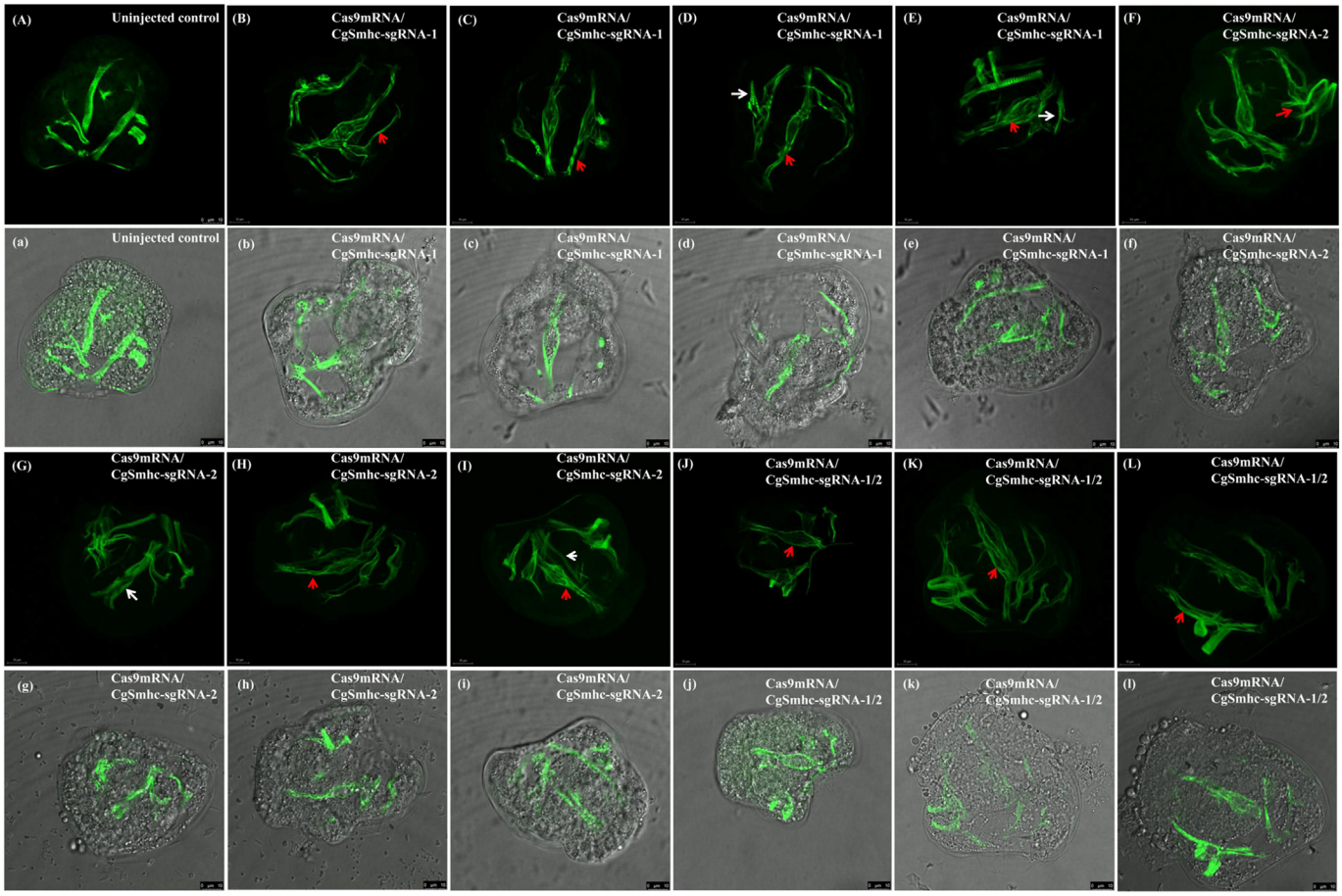

Fig. 6. A(a): The musculature of uninjected larvae; B–E(b–e): The musculature of larvae injected with CgSmhc-sgRNA-1/Cas9 mRNA; F–I(f–i): The musculature of larvae injected with CgSmhc-sgRNA-2/Cas9 mRNA; J–L(j–l): The musculature of larvae injected with CgSmhc-sgRNA-1/2/Cas9 mRNA. The red arrows indicate that the sarcomere was disrupted; the white arrows indicate that the sarcomere was assembled correctly. Dual sgRNAs injections not only resulted in an increased proportion of larvae showing sarcomere defection, but also increased the degree of sarcomere abnormality.

4.6. Functional analysis of CgSmhc in larval myogenesis and motor ability

To further verify the function of CgSmhc in larval myogenesis, CgSmhc was knockout by CRISPR/Cas9 system. Loss of CgSmhc had a visible effect on the sarcomeric organization of thin filaments in larval musculature. Targeted mutation of CgSmhc abolished sarcomere organization in larval velum retractor, indicating that CgSmhc was involved in larval myogenesis and played a crucial regulatory role in sarcomere assembly of muscle in *C. gigas*. We speculated that loss of CgSmhc resulted in the structural or functional disruption of myosin, which was the key component of sarcomere [2]. Similarly, knockdown or knockout of slow myosin heavy chain 1 resulted in defective sarcomere organization in embryonic slow muscles in zebrafish [12,55].

Knockout of CgSmhc resulted in a significant reduction of larval motor ability, suggesting that CgSmhc was a key regulator of larval locomotion in *C. gigas*. The sarcomere was the basic contractile unit in skeletal muscle, and the musculature was the primary motor organ of larvae in *C. gigas* [55]. Therefore, we speculated that reduction of larval locomotion was for the reason that loss of CgSmhc resulted in the abolish of sarcomere and the disruption of muscle contraction ability. The results suggested that CgSmhc was involved in the muscle contraction in *C. gigas*. This was consistent with previous report that MyHC-IIb null mice showed a significantly reduced levels of muscle contractile force [56].

Table 2
The larval hatching rate in wild type and injected larvae.

Uninjected control			Cas9mRNA/CgSmhc-sgRNA1/2 injection		
One-cell embryos (number)	D-shaped larvae (number)	Hatching rate (%)	One-cell embryos (number)	D-shaped larvae (number)	Hatching rate (%)
338	105	31%	301	35	12%
486	133	27%	194	15	7%
468	223	47%	155	37	23%
300	102	34%	150	18	12%

Supplementary data to this article can be found online at https://doi.org/10.1016/j.ijbiomac.2021.03.022.

CRediT authorship contribution statement

Huijuan Li: Investigation, Methodology, Formal analysis, Writing-original draft.

Hong Yu: Methodology, Formal analysis, Writing - review & editing. Shaojun Du: Methodology, Conceptualization, Writing - review & editing. Qi Li: Conceptualization, Funding acquisition, Supervision, Writing - review & editing.

Acknowledgements

This study was supported by grants from the National Key Research and Development Program of China (2018YFD0900200), National Natural Science Foundation of China (31672649), Weihai Science and Technology Development Program (2018NS01), and Industrial Development Project of Qingdao City (20-3-4-16-nsh).

References

[1] J. Xu, J. Gao, J. Li, L. Xue, K.J. Clark, S.C. Ekker, S.J. Du, Functional analysis of slow myosin heavy chain 1 and myomesin-3 in sarcomere organization in zebrafish embryonic slow muscles, J. Genet. Genomics 39 (2012) 69–80.

[2] E. Ehler, M. Gautel, The sarcomere and sarcomerogenesis, Adv. Exp. Med. Biol. 642 (2008) 1–14.

[3] W.F. Harrington, M.E. Rodgers, Myosin, Rev. Biochem. 53 (1984) 35–73.

[4] C. Reggiani, S. Schiaffino, Molecular diversity of myofibrillar proteins: gene regulation and functional significance, Physiol. Rev. 76 (1996) 371–423.

[5] M.J. Cope, J. Whisstock, I. Rayment, J. Kendrick-Jones, Conservation within the myosin moter domain: implications for structure and function, Structure 4 (1996) 969–987.

[6] M. Periasamy, R.M. Wydro, M.A. Strehler-Page, E.E. Strehler, B. Nadal-Ginard, Characterization of cDNA and genomic sequences corresponding to an embryonic myosin heavy chain, J. Biol. Chem. 260 (1985) 15856–15862.

[7] G.E. Lyons, M. Ontell, R. Cox, D. Sassoon, M. Buckingham, The expression of myosin genes in developing skeletal muscle in the mouse embryo, J. Cell Biol. 111 (1990) 1465–1476.

[8] C. DeNardi, S. Ausoni, P. Moretti, Type 2X myosin heavy chain is coded by a muscle fiber type specific and developmentally regulated gene, J. Cell Biol. 123 (1993) 823–835.

[9] M. Barany, ATPase activity of myosin correlated with speed of muscle shortening, J. Gen. Physiol. 50 (1967) 197–218.

[10] A. Sharma, M. Agarwal, A. Kumar, P. Kumar, M. Saini, G. Kardon, S.J. Mathew, Myosin heavy chain-embryonic is a crucial regulator of skeletal muscle development and differentiation, BioRxiv (2018) 261685.

[11] L.J. Acakpo-Satchivi, W. Edelmann, C. Sartorius, B.D. Lu, P.A. Wahr, S.C. Watkins, J.M. Metzger, L. Leinwand, R. Kucherlapati, Growth and muscle defects in mice lacking adult myosin heavy chain genes, J. Cell Biol. 139 (1997) 1219–1229.

[12] S.P. Li, H. Wen, S. Du, Defective sarcomere organization and reduced larval locomotion and fish survival in slow muscle heavy chain 1 (smyhc1) mutants, FASEB 34 (1) (2020) 1378–1397.

[13] A.K.S. Ahammad, M. Asaduzzaman, S. Asakawa, Regulation of gene expression mediating indeterminate muscle growth in teleosts, Mech. Dev. 137 (2015) 53–65.

[14] L. Nyitray, E.B. Goodwin, A.G. Szent-Gyo¨rgyi, Complete primary structure of a scallop striated muscle myosin heavy chain. Sequence comparison with other heavy chains reveals regions that might be critical for regulation, J. Biol. Chem. 266 (1991) 18469–18476.

[15] Y. Hasegawa, Complete nucleotide sequence of a cDNA encoding a myosin heavy chain from mantle tissue of scallop *Patinopecten yessoensis*, Fish. Sci. 68 (2002) 403–415.

[16] D.P. Janes, H. Patel, P.D. Chantler, Primary structure of myosin from the striated adductor muscle of the Atlantic scallop,*Pecten maximus*, and expression of the regulatory domain, J. Muscle Res. Cell Motil. 21 (2000) 415–422.

[17] C.L. Perreault-Micale, V.N. Kalabokis, L. Nyitray, A.G. SzentGyo¨rgyi, Sequence variations in the surface loop near the nucleotide binding site modulate the ATP turnover rates of molluscan myosins, J. Muscle Res. Cell Motil. 17 (1996) 543–553.

[18] K. Matulef, K. Sirokman, C.L. Perreault-Micale, A.G. SzentGyo¨rgyi, Amino-acid sequence of squid myosin heavy chain, J. Muscle Res. Cell Motil. 19 (1998) 705–712.

[19] K. Caldeira, M.E. Wickett, Oceanography: anthropogenic carbon and ocean pH, Nature 425 (2003) 365.

[20] Y. Tsutsui, M. Yoshio, K. Oiwa, A. Yamada, Striated muscle twitchin of bivalves has “catchability”, the ability to bind thick filaments tightly to thin filaments, representing the catch state, J. Mol. Biol. 365 (2007) 325–332.

[21] H.J. Li, H. Yu, S.J. Du, Q. Li, Developmental dynamics of myogenesis in pacific oyster *Crassostrea gigas*, Comp. Biochem. Physiol. B Biochem. Mol. Biol. 227 (2019) 21–30.

[22] J.M. Bono, E.C. Olesnicky, L.M. Matzkin, Connecting genotypes, phenotypes and fitness: harnessing the power of CRISPR/Cas9 genome editing, Mol. Ecol. 24 (2015) 3810–3822.

[23] T.J. Cradick, E.J. Fine, C.J. Antico, G. Bao, CRISPR/Cas9 systems targeting β-globin and CCR5 genes have substantial off-target activity, Nucleic Acids Res. 41 (2013) 9584–9592.

[24] N. Chang, C. Sun, L. Gao, Genome editing with RNA-guided Cas9 nuclease in zebrafish embryos, Cell Res. 23 (2013) 465–472.

[25] L. Cong, F.A. Ran, D. Cox, S. Lin, R. Barretto, N. Habib, F. Zhang, Multiplex genome engineering using CRISPR/Cas systems, Science 339 (2013) 819–823.

[26] J.A. Doudna, E. Charpentier, The new frontier of genome engineering with CRISPR-Cas9, Science 346 (2014) 1258096.

[27] T. Momose, J.P. Concordet, Diving into marine genomics with CRISPR/Cas9 systems, Mar. Genomics 30 (2016) 55–65.

[28] C.N.T. Taning, B. Van Eynde, N. Yu, CRISPR/Cas9 in insects: applications, best practices and biosafety concerns, J. Insect Physiol. 98 (2017) 245–257.

[29] S.M. Sanders, Z. Ma, J.M. Hughes, CRISPR/Cas9-mediated gene knock-in in the hydroid *Hydractinia symbiolongicarpus*, BMC Genomics 19 (2018), 649, .

[30] H. Yu, H. Li, Q. Li, R. Xu, S. Du, Targeted gene disruption in pacific oyster based on crispr/cas9 ribonucleoprotein complexes, Mar. Biotechnol. 21 (2019) 301–309.

[31] X. Robert, P. Gouet, Deciphering key features in protein structures with the new ENDscript server, Nucleic Acids Res. 42 (2014) 320–324.

[32] S. Kumar, G. Stecher, K. Tamura, MEGA7: molecular evolutionary genetics analysis version 7.0 for bigger datasets, Mol. Biol. Evol. 33 (2016) 1870–1874.

[33] Y. Du, L. Zhang, F. Xu, B. Huang, G. Zhang, L. Li, Validation of housekeeping genes as internal controls for studying gene expression during Pacific oyster (*Crassostrea gigas*) development by quantitative real-time PCR, Fish Shellfish Immunol. 24 (2013) 939–945.

[34] C. Thisse, B. Thisse, High resolution in situ hybridization on whole-mount zebrafish embryo, Nat. Protoc. 3 (2008) 59–69.

[35] Q. Li, A. Kijima, Segregation of microsatellite alleles in gynogenetic diploid Pacific abalone (*Haliotis discus hannai*), Mar. Biotechnol. 7 (6) (2005) 669.

[36] S. Galler, T.L. Schmitt, D. Pette, Stretch activation, unloaded shortening velocity, and myosin heavy chain isoforms of rat skeletal muscle fibers, J. Physiol. 478 (1994) 513–521.

[37] S. Schiaffino, C. Reggiani, Molecular diversity of myofibrillar proteins: gene regulation and functional significance, Physiol. Rev. 76 (1996) 371–423.

[38] R.E. Cheney, M.S. Mooseker, Unconventional myosins, Curr. Opin. Cell Biol. 4 (1) (1992) 27.

[39] A.G. Szent-Györgyi, V.N. Kalabokis, C.L. Perreault-Micale, Regulation by molluscan myosins, Mol. Cell. Biochem. 190 (1999) 55–62.

[40] E. Emanuel, Marie-Antoinette Strehler, Strehler-Page, Complete nucleotide and encoded amino acid sequence of a mammalian myosin heavy chain gene: evidence against intron-dependent evolution of the rod, J. Mol. Biol. 190 (3) (1986) 291–317.

[41] H. Yu, H.J. Li, Q. Li, Molecular characterization and expression profiles of myosin essential light chain gene in the Pacific oyster *Crassostrea gigas*, Comp. Biochem. Physiol. B Biochem. Mol. Biol. 213 (2017) 1–7.

[42] V. Dyachuk, N. Odintsova, Development of the larval muscle system in the mussel *Mytilus trossulus* (Mollusca, Bivalvia), Develop. Growth Differ. 51 (2) (2009) 69–79.

[43] P.D. Wagner, E. Giniger, Hydrolysis of ATP and reversible binding to F-actin by myosin heavy chains free of all light chains, Nature 292 (1981) 560–562.

[44] M. Sivaramakrishnan, M. Burke, The free heavy chain of vertebrate skeletal myosin subfragment 1 shows full enzymatic activity, J. Biol. Chem. 257 (1982) 1102–1105.

[45] T.G. Dix, Histology of the mantle and pearl sac of the pearl oyster *Pinctada Maxima* (Lamellibranchia), Molluscan. Res. 2 (4) (1973) 365–375.

[46] S.T. Smale, J.T. Kadonaga, The RNA polymerase II core promoter, Annu. Rev. Biochem. 72 (2003) 449–479.

[47] Y. Liang, J. Cui, G. Yang, Polymorphisms of 5′ flanking region of chicken prolactin gene, Domest. Anim. Endocrinol. 30 (1) (2006) 1–16.

[48] A.S. Ahammad, M. Asaduzzaman, S. Asakawa, S. Watabe, S. Kinoshita, Regulation of gene expression mediating indeterminate muscle growth in teleosts, Mech. Dev. 137 (2015) 53–65.

[49] B. Camoretti-Mercado, N.O. Dulin, J. Solway, Serum response factor function and dysfunction in smooth muscle, Respir. Physiol. Neurobiol. 137 (2003) 223–235.

[50] J.M. Miano, Serum response factor: toggling between disparate programs of gene expression, J. Mol. Cell. Cardiol. 35 (2003) 577–593.

[51] D.L. Allen, J.N. Weber, L.K. Sycuro, L.A. Leinwand, Myocyte enhancer factor-2 and serum response factor binding elements regulate fast myosin heavy chain transcription in vivo, J. Biol. Chem. 280 (2005) 17126–17134.

[52] M. Asaduzzaman, S. Kinoshita, B.S. Siddique, S. Asakawa, S. Watabe, Multiple cis-elements in the 5′-flanking region of embryonic/larval fast-type of the myosin heavy chain gene of torafugu, myh(m743-2), function in the transcriptional regulation of its expression, 489 (1) (2011) 41–54.

[53] A. Kobiyama, M. Hirayama, M. Muramatsu-Uno, S. Watabe, Functional analysis on the 5′-flanking region of carp fast skeletal myosin heavy chain genes for their expression at different temperatures, Gene 372 (2006) 82–91.

[54] C.S. Liang, D. Ikeda, S. Kinoshita, A. Shimizu, T. Sasaki, S. Asakawa, Myocyte enhancer factor 2 regulates expression of medaka oryzias latipes fast skeletal myosin heavy chain genes in a temperature-dependent manner, Gene 407 (2008) 42–53.

[55] J. Xu, J. Gao, J.L. Li, L.Y. Xue, K.J. Clark, S.C. Ekker, S.J. Du, Functional analysis of slow myosin heavy chain 1 and myomesin-3 in sarcomere organization in zebrafish embryonic slow muscles, J. Genet. Genomics 39 (2) (2012) 69–80.

[56] L.J. Acakpo-Satchivi, W. Edelmann, C. Sartorius, B.D. Lu, P.A. Wahr, S.C. Watkins, J.M. Metzger, L. Leinwand, R. Kucherlapati, Growth and muscle defects in mice lacking adult myosin heavy chain genes, J. Cell Biol. 139 (1997) 1219–1229.